

usually anticipated that chemical synthesis methods such as COPPT will produce a material exhibiting better phase and chemical purity than materials produced with more conventional methods such as SSS or HET. In this case, however, formation and decomposition of $\text{Ba}_2\text{Y}_2\text{O}_5\cdot 2\text{CO}_2$ kinetically limited the formation of $\text{Ba}_4\text{Y}_2\text{O}_7\cdot \text{CO}_2$. Thus, intermediate $\text{Ba}_2\text{Y}_2\text{O}_5\cdot 2\text{CO}_2$ formation served to segregate the powder mixtures regardless of the mixing structure existing as a result of the processing method. Intermediate compound formation of this type has been observed in the preparation of Ba_2SiO_4 from BaCO_3 - SiO_2 mixtures,³⁰ in which BaSiO_3 was the intermediate compound found to coexist with BaCO_3 . In that case, Ba_2SiO_4 began to form only after complete consumption of the SiO_2 . Similar solid-state chemistry has been observed in the synthesis of β -wollastonite.³¹

In the preparation of $\text{Ba}_4\text{Y}_2\text{O}_7\cdot \text{CO}_2$, formation of the intermediate phase $\text{Ba}_2\text{Y}_2\text{O}_5\cdot 2\text{CO}_2$ was also independent of the synthesis method. This indicates that the reaction kinetics of $\text{Ba}_2\text{Y}_2\text{O}_5\cdot 2\text{CO}_2$ was not controlled by the diffusion rate of reactant species but instead by factors that influence the nucleation and/or growth of the $\text{Ba}_2\text{Y}_2\text{O}_5\cdot 2\text{CO}_2$ phase. For instance, nucleation site density for $\text{Ba}_2\text{Y}_2\text{O}_5\cdot 2\text{CO}_2$ could strongly influence the nucleation rate, and this parameter can be independent of the character-

istics of the powder. Rate-limiting product nucleation has been observed in solid-state reactions between BaCO_3 and ZnO .³²

Conclusions

Solid-state reaction of individual powders prepared by SSS, HET, and COPPT methods produced a $\text{Ba}_4\text{Y}_2\text{O}_7\cdot \text{CO}_2$ powder with similar characteristics. The optimal reaction conditions for formation of $\text{Ba}_4\text{Y}_2\text{O}_7\cdot \text{CO}_2$ were a 20-h soak at 1050 °C. The reaction conditions were found to be independent of the preparation method, due to the formation of the $\text{Ba}_2\text{Y}_2\text{O}_5\cdot 2\text{CO}_2$ intermediate phase in all systems. Formation of $\text{Ba}_2\text{Y}_2\text{O}_5\cdot 2\text{CO}_2$ was also independent of the synthesis method and was controlled instead by factors such as nucleation site density, which can be independent of the powder characteristics or mixedness.

Acknowledgment. We acknowledge the generous support of Engelhard Corp., the New Jersey State Commission on Science and Technology, and the Center for Ceramic Research. The assistance of Ms. K. Griffin in the preparation of the manuscript is gratefully appreciated.

Registry No. Y_2O_3 , 1314-36-9; $(\text{NH}_2)\text{CO}$, 57-13-6; YOHCO_3 , 136632-09-2; $\text{Ba}(\text{CO}_3)$, 513-77-9; $\text{Ba}(\text{NO}_3)_2$, 10022-31-8; $\text{Y}(\text{NO}_3)_3$, 10361-93-0; NH_4HCO_3 , 1066-33-7; $\text{Y}_2(\text{CO}_3)_2\text{NO}_3\text{OH}$, 136826-97-6; $\text{Ba}_4\text{Y}_2\text{O}_7\cdot \text{CO}_2$, 117128-24-2; $\text{Ba}_2\text{Y}_2\text{O}_5$, 11071-75-3; BaO , 1304-28-5; $\text{Ba}_2\text{Y}_2\text{O}_5\cdot 2\text{CO}_2$, 117128-25-3; BaO_2 , 1304-29-6.

(30) Yamaguchi, T.; Fujii, H.; Kuno, H. *J. Inorg. Nucl. Chem.* 1972, 34, 2739.

(31) Ibanez, A.; Gonzalez Pena, J. M.; Sandoval, F. *Am. Ceram. Soc. Bull.* 1990, 69, 374.

(32) Hulbert, S. F.; Klawitter, J. J. *J. Am. Ceram. Soc.* 1967, 50, 484.

Ordered Bimetallic-Radical Species Forming Low-Dimensional Magnetic Materials

Andrea Caneschi,[†] Dante Gatteschi,^{*,†} Paul Rey,[†] and Roberta Sessoli[†]

Department of Chemistry, University of Florence, via Maragliano 75, Florence, Italy, and Centre d'Etudes Nucleaires, Grenoble, France

Received June 11, 1991. Revised Manuscript Received October 24, 1991

2-(4-Pyridyl)-4,4,5,5-tetramethylimidazoline-1-oxyl 3-oxide, NITpPy, reacts with metal hexafluoroacetylacetonates, $\text{M}(\text{hfac})_2$, forming compounds of formula $\text{Mn}_2\text{M}(\text{hfac})_6(\text{NITpPy})_2$, with $\text{M} = \text{Mn}, \text{Co}, \text{Ni}$. No crystals suitable for X-ray analysis could be obtained, but powder diffraction data suggested that all the compounds are isomorphous. On the basis of magnetic and IR evidence, we assume that in all these compounds $\text{Mn}(\text{hfac})_2(\text{NITpPy})$ chains are present in which the radicals bridge two manganese(II) ions through the NO groups. The pyridine nitrogen donors bind the M atoms to connect different chains. In this way either ladders or two-dimensional structures can be formed. All the compounds order magnetically below 10 K, giving rise to spontaneous magnetization.

Introduction

Magnetic molecular materials have been the object of increasing interest in the last few years. In fact these systems can potentially associate bulk ferro- or ferrimagnetism or weak ferromagnetism with chemical and optical properties typical of molecular compounds and eventually they can be exploited in devices. Currently several different synthetic approaches are followed in order

to synthesize this type of material,¹ which can be classified as organic,² organic-organometallic,³ organic-inorganic,⁴

(1) *Magnetic Molecular Materials*; Gatteschi, D., Kahn, O., Miller, J. S., Palacio, F., Eds.; Kluwer: Dordrecht, The Netherlands, 1991.

(2) Sugawara, T.; Bandow, S.; Kimura, K.; Iwamura, H.; Itoh, K. *J. Am. Chem. Soc.* 1986, 108, 368. Dougherty, D. A. *Mol. Cryst. Liq. Cryst.* 1989, 176, 25. Veciana, J.; Rovira, C.; Armet, O.; Domingo, V. M.; Crespo, M. I.; Palacio, F. *Mol. Cryst. Liq. Cryst.* 1989, 176, 77. Le Page, T. J.; Breslow, R. *J. Am. Chem. Soc.* 1987, 109, 6412. Torrance, J. B.; Bagus, P. S.; Johannsen, I.; Nazzari, A. I.; Parkin, S. S. P. *J. Appl. Phys.* 1988, 63, 2962.

[†]University of Florence.

^{*}Centre d'Etudes Nucleaires.

and inorganic⁵ according to the chemical nature of the magnetic centers which are used in order to assemble the three-dimensional structure.

Encouraging results have been obtained, but it is clear that if the critical temperatures to three-dimensional order must be substantially increased, it is necessary to develop new materials which have strong interactions not only in one direction, as achieved so far, but also in two other directions. Recently promising results have been obtained along these lines by dehydrating one-dimensional materials in order to increase the interactions between chains.^{6,7}

We have used nitronyl nitroxides, NITR, as ligands toward transition-metal⁴ and lanthanide⁸ ions, synthesizing one-dimensional ferro- and ferrimagnets. Although strong intrachain interactions are present in one-dimensional ferrimagnets, the interchain interactions are so weak that the magnetic order is driven by the dipolar interactions.

In order to increase the critical temperatures, we are currently trying to introduce in the NITR radicals substituent groups which contain additional donor atoms. In particular we synthesized the radical 2-(4-pyridyl)-4,4,5,5-tetramethylimidazoline-1-oxyl 3-oxide, NITpPy, which is potentially tridentate, with the hope that it might be possible to obtain materials in which chains are formed through a N-O-M-O-N network and are cross-linked through M'(py)₂ connections.

We previously reported that in simple complexes of formula M(hfac)₂(NITpPy)₂ (M = Mn, Ni),⁹ CuCl₂(NITpPy)₂,¹⁰ or MCl₂(NITpPy)₄ (M = Mn, Ni)⁹ the radical is magnetically coupled to the metal ion when it binds through the pyridine nitrogen. In particular the exchange coupling constant was found to be $J \approx -1 \text{ cm}^{-1}$ for manganese(II), $J \approx 20 \text{ cm}^{-1}$ for copper(II), and $J \approx 10 \text{ cm}^{-1}$ for nickel(II). We use the spin Hamiltonian in the form $\mathcal{H} = JS_1 \cdot S_2$. However in these compounds the radical acts as either monodentate or bidentate, rather than tridentate, and discrete, not extended, systems are obtained.

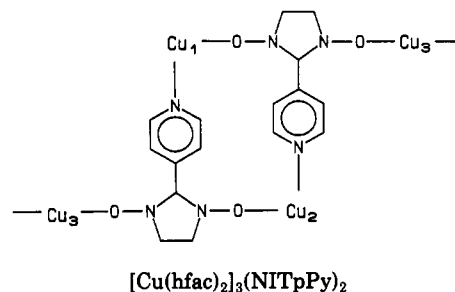
An extended system is present in [Cu(hfac)₂]₃(NITpPy)₂, where the radical acts as a tridentate ligand.¹¹ This

Table I. Absorption Frequencies in the Far-IR Spectra

compound	chromophore	$\nu(\text{M-O})^a$	$\nu(\text{M-N})^a$
I	?	340, 311	228, 179
II	?	313	223
III	?	310	223
Mn(hfac) ₂ (NITpPy) ₂	MnO ₄ N ₂	313	180
Co(hfac) ₂ (NITpPy) ₂	CoO ₄ N ₂	318	215
Ni(hfac) ₂ (NITpPy) ₂	NiO ₄ N ₂	324	236

^a In cm⁻¹.

compound behaves as a one-dimensional antiferromagnet, and our attempts to synthesize a two-dimensional magnetic material failed again.



We have now synthesized compounds of formula Mn₂M(hfac)₆(NITpPy)₂, where M = Mn, Co, Ni, which order magnetically at low temperature. Although we did not succeed in growing suitable crystals for X-ray analysis, we wish to report here the results of the investigation of their magnetic properties which provided us evidence of an extended structure determining a magnetic phase transition at low temperature.

Experimental Section

Synthesis of the Complexes. The three compounds Mn₂M(hfac)₆(NITpPy)₂ (M = Mn, Co, and Ni) were prepared by following the same procedure. M(hfac)₂·2H₂O as well as the NITpPy radical were prepared as previously described.^{12,13} Mn(hfac)₂·H₂O (0.5 mmol) and 0.25 mmol of M(hfac)₂·2H₂O, where M = Mn, Ni, and Co, were dissolved in boiling *n*-heptane. The solutions were cooled down to 80 °C and 0.5 mmol of NITpPy dissolved in CHCl₃ was added. The solutions were allowed to cool down slowly, and after 1 day, green crystalline products were collected. Anal. Calcd for Mn₃C₅₄H₃₈N₆O₁₆F₃₆: Mn, 8.78; C, 34.57; H, 2.04; N, 4.48. Found: Mn, 8.68; C, 34.62; H, 2.07; N, 4.38. Anal. Calcd for Mn₂CoC₅₄H₃₈N₆O₁₆F₃₆: Mn, 5.84; Co, 3.14; C, 34.50; H, 2.04; N, 4.47. Found: Mn, 5.94; Co, 3.06; C, 34.58; H, 2.11; N, 4.45. Anal. Calcd for Mn₂NiC₅₄H₃₈N₆O₁₆F₃₆: Mn, 5.85; Ni, 3.12; C, 34.51; H, 2.04; N, 4.47. Found: Mn, 5.96; Ni, 3.06; C, 34.54; H, 2.02; N, 4.45.

Physical Measurements. IR spectra were recorded with a Bruker IFS 113v Fourier transform spectrometer in the 400–40 cm⁻¹ region using polyethylene pellets.

A crystal of Mn₂Ni(hfac)₆(NITpPy)₂ was mounted on a CAD4 Enraf Nonius four-circle diffractometer equipped with Mo K α radiation. The quality of the crystal was very poor and reflections were collected only for $2\theta \leq 30^\circ$. X-ray powder spectra were recorded with a Philips diffractometer equipped with Co K α radiation.

The magnetic susceptibility of polycrystalline powder samples in the temperature range 2–300 K at a field strength of 10 mT as well as magnetization in variable fields were measured by an SHE SQUID magnetometer. Magnetization curves were obtained by using the same equipment.

Low field measurements were performed on a laboratory-assembled AC susceptometer based on a mutual inductance bridge

(3) Miller, J. S.; Epstein, A. J.; Reiff, W. M. *Chem. Rev.* **1988**, *88*, 201. Miller, J. S.; Epstein, A. J. *Mol. Cryst. Liq. Cryst.* **1989**, *176*, 347. Miller, J. S.; Calabrese, J. C.; Rommelmann, H.; Chittipeddi, S.; Zhang, J. H.; Reiff, W. M.; Epstein, A. J. *J. Am. Chem. Soc.* **1987**, *109*, 769. Broderick, W. E.; Thompson, J. A.; Day, E. P.; Hoffman, B. M. *Science* **1990**, *249*, 401.

(4) Caneschi, A.; Gatteschi, D.; Rey, P.; Sessoli, R. *Acc. Chem. Res.* **1989**, *22*, 392. Caneschi, A.; Gatteschi, D.; Rey, P.; Sessoli, R. *Inorg. Chem.* **1988**, *27*, 1756. Caneschi, A.; Gatteschi, D.; Renard, J.-P.; Rey, P.; Sessoli, R. *Inorg. Chem.* **1989**, *28*, 3914.

(5) Gleizes, A.; Verdaguer, M. *J. Am. Chem. Soc.* **1984**, *106*, 3727. Pei, Y.; Verdaguer, M.; Kahn, O.; Sletten, J.; Renard, J.-P. *Inorg. Chem.* **1987**, *26*, 138. Coronado, E.; Drillon, M.; Nutgeren, P. R.; de Jongh, L. J.; Beltran, D. *J. Am. Chem. Soc.* **1988**, *110*, 3907.

(6) Nakatani, K.; Carriat, J. Y.; Journaux, Y.; Kahn, O.; Lloret, F.; Renard, J.-P.; Pei, Y.; Sletten, J.; Verdaguer, M. *J. Am. Chem. Soc.* **1989**, *111*, 5739.

(7) Coronado, E.; Sapiña, F.; Beltran, D.; Burriel, R.; Carlin, R. L. *Mol. Cryst. Liq. Cryst.* **1989**, *176*, 507. Sapiña, F.; Coronado, E.; Gomez-Romero, P.; Beltran, D.; Burriel, R.; Carlin, R. L. *J. Appl. Phys.* **1990**, *67*, 6003.

(8) Benelli, C.; Caneschi, A.; Fabretti, C. A.; Gatteschi, D.; Pardi, L. *Inorg. Chem.* **1990**, *29*, 4153. Benelli, C.; Caneschi, A.; Gatteschi, D.; Pardi, L.; Rey, P. *Inorg. Chem.* **1990**, *29*, 4223. Benelli, C.; Caneschi, A.; Gatteschi, D.; Guillou, O.; Pardi, L. *Inorg. Chim. Acta* **1989**, *160*, 1. Benelli, C.; Caneschi, A.; Gatteschi, D.; Laugier, J.; Rey, P. *Angew. Chem., Int. Ed. Engl.* **1987**, *26*, 913.

(9) Caneschi, A.; Ferraro, F.; Gatteschi, D.; Rey, P.; Sessoli, R. *Inorg. Chem.* **1990**, *29*, 4217.

(10) Caneschi, A.; Ferraro, F.; Gatteschi, D.; Rey, P.; Sessoli, R. *Inorg. Chem.* **1990**, *29*, 1756.

(11) Caneschi, A.; Ferraro, F.; Gatteschi, D.; Rey, P.; Sessoli, R. *Inorg. Chem.* **1991**, *30*, 3162.

(12) Cotton, F. A.; Holm, R. H. *J. Am. Chem. Soc.* **1960**, *82*, 2979.

(13) Ullman, E. F.; Call, L.; Osiecki, J. H. *J. Org. Chem.* **1970**, *35*, 3623. Davis, M. S.; Morokuma, K.; Kreilick, R. W. *J. Am. Chem. Soc.* **1972**, *94*, 5588.

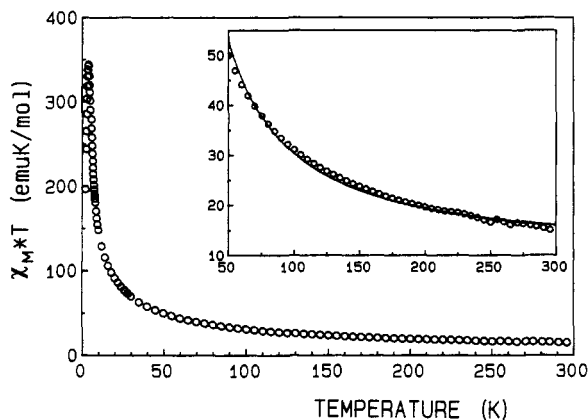


Figure 1. Temperature dependence of the magnetic susceptibility of $\text{Mn}_3(\text{hfac})_6(\text{NITpPy})_2$ in χT form. In the inset the solid line represents the values calculated as described in the text.

measuring both the real and imaginary component of the magnetic susceptibility. The sample was introduced in a fused silica Dewar vessel immersed in liquid helium. Low-pressure helium gas kept a weak thermal contact with the cryogenic bath. The temperature was measured with a calibrated gallium–aluminum arsenide diode placed on the sample. The measurements were performed at frequencies in the range 50–500 Hz in zero applied static field with an alternating field of 0.08 mT.

Electron paramagnetic resonance (EPR) spectra were recorded with a Varian E9 spectrometer at X-band frequency. Variable temperature spectra in the range 4.2–300 K were recorded by using an Oxford Instruments ESR9 liquid-helium continuous-flow cryostat.

Results

Synthesis of the Compounds. Compounds $\text{Mn}_2\text{Mn}(\text{hfac})_6(\text{NITpPy})_2$ (I), $\text{Mn}_2\text{Co}(\text{hfac})_6(\text{NITpPy})_2$ (II), and $\text{Mn}_2\text{Ni}(\text{hfac})_2(\text{NITpPy})_2$ (III) were synthesized by simply admixing solutions of $\text{Mn}(\text{hfac})_2 \cdot 2\text{H}_2\text{O}$, $\text{M}(\text{hfac})_2 \cdot 2\text{H}_2\text{O}$, and NITpPy. Crystalline material, but no really good crystals, was obtained. In the case of III, some seemingly good crystals were collected from a batch, but X-ray data revealed that they are actually very poor and the collected data did not allow us to solve the structure. However it was possible to determine a monoclinic unit cell of dimensions $a = 26.37 \text{ \AA}$, $b = 20.43 \text{ \AA}$, $c = 31.09 \text{ \AA}$, and $\beta = 111.3^\circ$. X-ray powder diffractograms of the three compounds showed only few well-resolved peaks.¹⁴ However the similarity of the three diffractograms suggests that they are all isomorphous.

In order to collect information on the binding of the radical to the metal ions, we recorded far-IR spectra of I–III and of $\text{M}(\text{hfac})_2(\text{NITpPy})_2$, $\text{M} = \text{Mn, Co, Ni}$, for comparison purposes. The results are shown in Table I. All the compounds have a band around 310 cm^{-1} , which can be attributed to a M–O stretching.^{15,16} The absorption at 180 cm^{-1} due to manganese–pyridine stretching^{17,18} is observed in I and in $\text{Mn}(\text{hfac})_2(\text{NITpPy})_2$, where manganese is known to be bound to pyridine, but not in II and III. In these compounds a band is observed at 223 cm^{-1} , which compares well with the metal–pyridine stretching

(14) The most intense peaks of the powder diffractograms: I, $2\theta = 7.2^\circ$ (Int = 100%), 14.4° (30%), 23.7° (20%); II, 7.25° (100%), 14.4° (25%), 23.7° (45%); III, 7.25° (100%); 14.4° (30%); 23.7° (30%).

(15) Kakiuti, Y.; Kida, S.; Quagliano, J. V. *Spectrochim. Acta* 1963, 19, 201.

(16) Thornton, D. A. *Coord. Chem. Rev.* 1990, 104, 173.

(17) Nakamoto, K. *Infrared and Raman Spectra of Inorganic and Coordination Compounds*; Wiley: New York, 1964.

(18) Thornton, D. A. *Coord. Chem. Rev.* 1990, 104, 251.

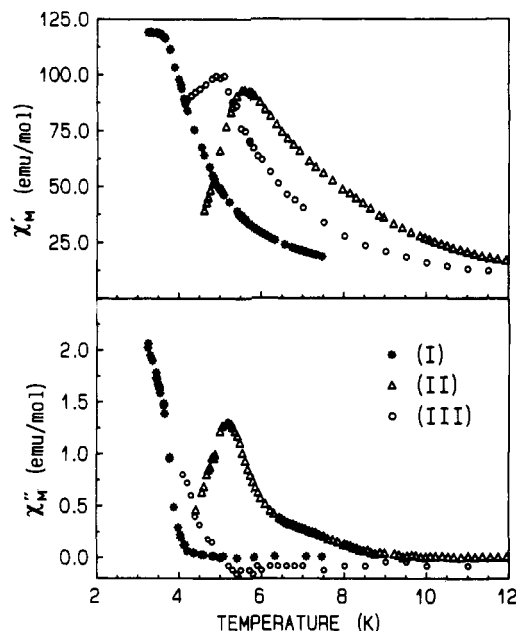


Figure 2. Real (top) and imaginary (bottom) components of the dynamic molar susceptibility of $\text{Mn}_3(\text{hfac})_6(\text{NITpPy})_2$ (*), $\text{Mn}_2\text{Co}(\text{hfac})_6(\text{NITpPy})_2$ (Δ), and $\text{Mn}_2\text{Ni}(\text{hfac})_6(\text{NITpPy})_2$ (O) measured in a field of 0.08 mT oscillating at 55 Hz. The value of χ'' of $\text{Mn}_2\text{Co}(\text{hfac})_6(\text{NITpPy})_2$ has been divided by a factor of 20 in order to fit the scale of the drawing.

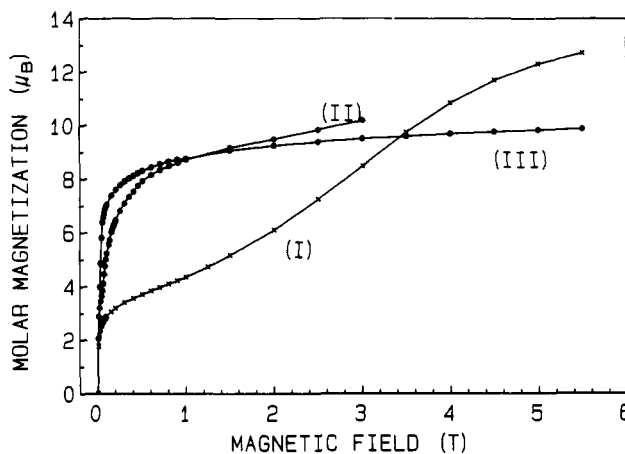


Figure 3. Molar magnetization of powder samples of $\text{Mn}_3(\text{hfac})_6(\text{NITpPy})_2$ (x), $\text{Mn}_2\text{Co}(\text{hfac})_6(\text{NITpPy})_2$ (O), and $\text{Mn}_2\text{Ni}(\text{hfac})_6(\text{NITpPy})_2$ (*) measured at 3.0 K. The lines are only a guide for the eye.

frequency observed in $\text{Ni}(\text{hfac})_2(\text{NITpPy})_2$ and $\text{Co}(\text{hfac})_2(\text{NITpPy})_2$.

Magnetic Properties. The temperature dependence of the dc χT product for $\text{Mn}_2\text{Mn}(\text{hfac})_6(\text{NITpPy})_2$ in an external field of 10 mT is shown in Figure 1. The room temperature value, $15.3 \text{ emu mol}^{-1} \text{ K}$, corresponding to $\mu_{\text{eff}} = 11.1 \mu_B$ per formula, is slightly higher than expected for uncorrelated spins, $13.5 \text{ emu mol}^{-1} \text{ K}$ ($10.4 \mu_B$). χT increases smoothly on decreasing temperature to a maximum of $344 \text{ emu mol}^{-1} \text{ K}$ ($52.5 \mu_B$) and then decreases.

Such high values of χT are a clear indication of short range magnetic order, and the low temperature decrease might be due to demagnetization effects. It is now well established that when such large χT values are observed, a magnetic phase transition can be suspected. Therefore we performed zero field ac susceptibility measurements at low temperature which showed a decrease of the real component of the susceptibility, χ' , and a concomitant onset of a nonzero imaginary component, χ'' , at ca. 4.2 K,

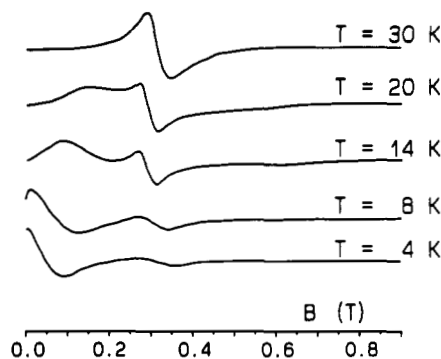


Figure 4. Powder X-band EPR spectra of I recorded at different temperatures. The resonance field of the standard (DPPH) is 0.3398 T.

as shown in Figure 2. The dc susceptibility remains almost constant below T_c as expected for an ordered ferromagnetic system.

Magnetization measurements were performed below the critical temperature at 3.0 K as shown in Figure 3. The experimental points can be grouped in four different regions within which linear variations of magnetization with external field are observed, with different slopes. At the lowest field, up to 50 mT, the slope is very steep, and the magnetization reaches ca. $3 \mu_B$. Above 50 mT, and up to 2 T, the slope is much flatter, indicating a first partial saturation region. Between 2 T and 4 T the slope increases again, and finally it tends to level off at higher fields. The highest value of the magnetization which we observed is ca. $13 \mu_B$.

Polycrystalline powder EPR spectra of I at room temperature show an isotropic signal at $g = 2$, with a peak-to-peak width of 60 G, plus a low intensity feature at $g = 4$. Short range order effects¹⁹ are clearly evidenced by the low-temperature spectra which show large shifts of the $g = 2$ resonance and a very marked anisotropy (Figure 4).

The temperature dependence of the magnetic susceptibility of $Mn_2Co(hfac)_6(NITpPy)_2$ is similar to that of $Mn_2Mn(hfac)_6(NITpPy)_2$. χT at room temperature is $14.1 \text{ emu mol}^{-1} \text{ K}$ ($10.6 \mu_B$). It increases to a maximum of $557.9 \text{ emu mol}^{-1} \text{ K}$ ($66.8 \mu_B$) at 4.5 K, and then decreases (Figure S1 in the supplementary material).

The ac susceptibility of II is completely different from that of I. The imaginary part χ'' , reported in Figure 2, becomes different from zero at ca. 10 K, while at this temperature χ' is still increasing. The value of χ'' is much larger than that observed in I and III and reaches a maximum at 5.2 K, while χ' goes through a maximum at 5.6 K. These values refer to the measurements performed at 55 Hz; the behavior remains substantially the same at higher frequency (500 Hz) but the temperatures of the two maxima slightly increase (6 K for χ' and 5.5 for χ'').

The magnetization of II measured at 3.0 K increases smoothly versus the field and then levels off at a value of ca. $9 \mu_B$ even if complete saturation is not achieved.

Polycrystalline powders of II are EPR silent at room temperature, but signals are observed below 30 K. At 4.2 K they show three features at $g \approx 1.3, 2.2$, and 8.8.

$Mn_2Ni(hfac)_6(NITpPy)_2$ has $\chi T = 13.9 \text{ emu mol}^{-1} \text{ K}$ at room temperature ($10.5 \mu_B$); it increases smoothly to a maximum of $48.6 \text{ emu mol}^{-1} \text{ K}$ at 4.5 K ($62.3 \mu_B$) and then decreases (Figure S2 in the supplementary material).

The ac susceptibility of III is similar to that of I. χ'' becomes different from zero at about 5 K where also a maximum in χ' is observed suggesting the presence of a

magnetic phase transition. As in I the dc susceptibility is almost constant below T_c .

The magnetization of III measured at 3.0 K increases rapidly in an external field and then saturates at a value of ca. $10 \mu_B$.

Polycrystalline powder EPR spectra of III at room temperature show one feature at $g = 2$, with a peak-to-peak width of 950 G. On cooling of the sample, the spectrum remains substantially unchanged down to ca. 30 K. Below this limit it becomes anisotropic and at 4.2 K the three g values are resolved: $g_1 = 7, g_2 = 2.2, g_3 = 1.6$.

The hysteresis loops of the three compounds were measured at 3 K with the SQUID magnetometer mentioned above. No hysteresis has been observed suggesting that the coercive field is smaller than 1 mT, the smallest field achieved by our apparatus. A small remanence perhaps has not been observed due to the rapid decay of residual magnetization which is often observed in soft magnetic material when T/T_c is not much smaller than 1.

Discussion

The lack of structural data obliges us to some speculation in order to interpret the observed magnetic properties. However a few points emerge clearly from the analysis of the magnetic properties and from the comparison with those previously reported for $M(hfac)_2(NITR)$ complexes.⁴ We will consider first $Mn_2Mn(hfac)_6(NITpPy)_2$.

The large effective magnetic moments and the g shifts in the paramagnetic phase are only compatible with low dimensional magnetic materials, while the onset of out-of-phase susceptibility in zero field indicates a magnetic phase transition.²⁰ Magnetic phase transitions are currently studied by ac susceptibility and an exhaustive treatment of the characterization of molecular magnetic materials by this technique can be found in ref 21.

The magnetization data below the phase transition show that the ordered state has a spontaneous magnetization, because it readily reaches a saturation value in a small external field. Since we could perform measurements only on polycrystalline samples where both easy and hard axes are present, the data can be used to conclude that magnetocrystalline anisotropy is small in this case.

The first saturation value observed, ca. $3 \mu_B$, is close to the value expected for $S = 3/2$. It cannot be exactly determined because higher fields determine a second slower increase of the magnetization up to ca. $12.5 \mu_B$, which reasonably agrees with a spin $S = 13/2$. The passage from the first to the second saturation value corresponds to the reversal of a $S = 5/2$ spin, with a behavior similar to that of metamagnets,^{20,22} but starting from a magnetic rather than from an antiferromagnetic state.

The indication of low-dimensional magnetic nature at high temperature, and the similarity of the magnetic data with those previously reported for $Mn(hfac)_2(NITR)$ derivatives,⁴ suggest a structure in which manganese ions are connected by μ -1,3 bridging radicals through the two N-O groups. The far-IR data on the other hand show that the pyridine nitrogen is also bound to manganese. We assume that this nitrogen is bound to a different manganese ion, which does not belong to the chain. This manganese ion must be bound to two pyridine rings to two radicals. A scheme of the proposed structure is shown in Figure 5a. It consists of ladders whose side pieces are formed by

(20) Carlin, R. L. *Magnetochemistry*; Springer-Verlag: Berlin, 1986.

(21) Palacio, F.; Lazaro, F. J.; van Duyneveldt, A. J. *Mol. Cryst. Liq. Cryst.* 1989, 176, 289.

(22) Stryjewski, E.; Giordano, N. *Adv. Phys.* 1977, 26, 487.

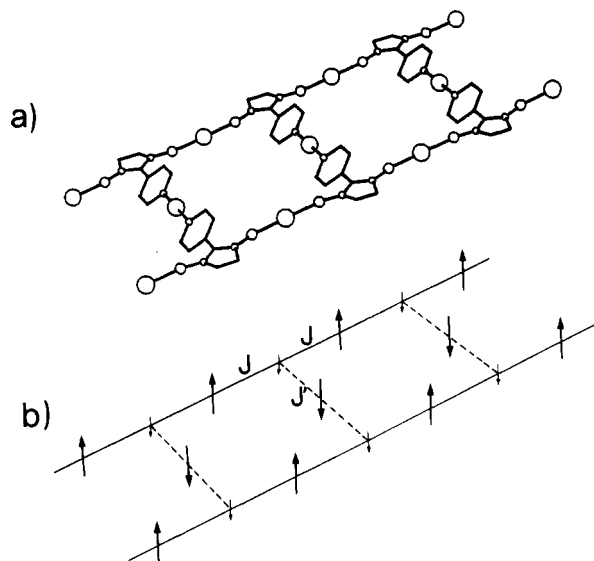


Figure 5. Schematic view of the structure postulated for the three derivatives (a) and suggested spin coupling scheme in $\text{Mn}_3(\text{hfac})_6(\text{NITpPy})_2$ (b).

$\text{Mn}(\text{hfac})_2(\text{NITpPy})_2$ chains and cross pieces by $\text{Mn}(\text{py})_2$ groups. The structure suggested in Figure 5 is not the only one which is compatible with the one-dimensional magnetic behavior. In fact the $\text{Mn}(\text{py})_2$ groups might connect a chain with two neighboring chains, instead of with one chain. This would be equivalent to have two successive cross-pieces stretching out in opposite directions. In this way layers instead of ladders would be formed similar to those observed²³ in $[\text{Mn}(\text{F}_5\text{prop})_2]_2(\text{NITMe})(\text{IMHMe})$ (F_5prop = pentafluoropropionate, IMHMe = 2,4,4,5,5-tetramethyl-4,5-dihydroimidazole 3-oxide). We cannot decide which of the two structures is the more probable. As far as the magnetic data are concerned, both provide qualitatively the same kind of interpretation, therefore in the following we will refer to the ladder structure, with the understanding that the same considerations might be used for the layer structure.

The previously reported data⁹ on the magnetic coupling in compounds containing manganese(II) and NITpPy suggests that the Mn–O bond corresponds to a strong antiferromagnetic interaction ($J \approx 300 \text{ cm}^{-1}$), while the Mn–N bond corresponds to a weak ferromagnetic interaction ($J' \approx -1 \text{ cm}^{-1}$). We consider therefore that at high temperature the two sides of the ladder are uncorrelated and the magnetic data should correspond to two substantially uncoupled manganese-radical chains plus the contribution of an isolated manganese ion. Deviations due to the coupling through the pyridine rings should start to show up only at relatively low temperatures.

In fact the observed temperature dependence of χT down to 50 K closely resembles that previously reported for $\text{Mn}(\text{hfac})_2(\text{NITR})$ linear chain compounds if allowance is made for the difference in molecular formula and the contribution of an uncorrelated manganese ion is added. The fitting of χT according to this assumption is shown in Figure 1. The best fit value of J , calculated for chains of alternating classic and quantum spins,²⁴ is $320 (3) \text{ cm}^{-1}$, in good agreement with the values previously reported for similar chains.⁴

If our assumption about the structure of $\text{Mn}_2\text{Mn}(\text{hfac})_6(\text{NITpPy})_2$ is correct, the inclusion of a ferromag-

netic J' yields at 0 K a preferred spin arrangement in the ladders as shown in Figure 5b. For the formula unit of $\text{Mn}_2\text{Mn}(\text{hfac})_6(\text{NITpPy})_2$, this corresponds to a ground $S = 3/2$ state. In fact the spins in the side pieces of the ladder correspond to $S = 4$, and the ferromagnetic coupling between a radical and the off-chain manganese on the cross-pieces keeps the spin of the latter reversed relative to the dominant manganese spins in the chain. On the contrary an antiferromagnetic coupling would keep the off-chains manganese spin parallel to those of the ions on the chains. Therefore with this spin topology we have the counterintuitive effect that ferromagnetic coupling gives a lower spin state than antiferromagnetic coupling.

The weak ferromagnetic coupling can be affected by the external field, finally reversing the off-chain manganese spin and orienting it parallel to the dominant spins. This simple model therefore is able to qualitatively account for many of the observed magnetic properties of I.

Our interpretation of the magnetic phase transition is that the spins of different ladders orient parallel to each other presumably due to dipolar interactions, as observed for other $\text{Mn}(\text{hfac})_2(\text{NITR})$ chains.⁴ The behavior of χ' and χ'' is typical of ferromagnets with low magnetic density and consequently large magnetic domains.²¹ The movements of the walls of these large domains in order to follow the oscillating field are almost impossible even at low frequency and a maximum in χ' occurs. On the contrary the dc susceptibility below T_c reaches a plateau corresponding to $1/N$, where N is the demagnetization factor, as expected for a ferromagnet.²⁵

Since the diffraction data seem to indicate that the nickel and cobalt derivatives are isomorphous, and presumably isostructural to the manganese, the same model should account also for the magnetic properties of the two former compounds. However, since they contain two different metal ions, several different possibilities arise. In fact Mn and M ions either may be randomly distributed along the side- and cross-pieces of the ladder or they may show site selectivity. In this case either the manganese or the M ions may prefer the side-pieces. The magnetic data, to be discussed in detail below, agree with an essentially order structure, and the far-IR data indicate that the M ions prefer the pyridine-coordinated site. This is in line with the softer character of nickel and cobalt compared to manganese.²⁶ Spontaneous resolution of different metal ions in different coordination sites is well documented in the EDTA class of one-dimensional bimetallic materials.²⁷

The ac susceptibility data clearly indicate a magnetic phase transition for both II and III at a higher temperature than for I. This is not compatible with a random distribution of the metal ions but strongly suggests an ordered structure. A second clear piece of evidence against a random distribution comes from the magnetization data: in fact if II and III were disordered, they should have some Mn_2Mn character which should show up in the magnetization curve. A simple look at the curves for II and III reveals that there is no resemblance to that of curve I.

The low-field magnetization of $\text{Mn}_2\text{Ni}(\text{hfac})_6(\text{NITpPy})_2$ agrees with a magnetically ordered state characterized by spontaneous magnetization with larger anisotropy com-

(25) Morrish, A. H. *The Physical Principles of Magnetism*; Krieger, R. E. Publ. Co.; New York, 1980.

(26) Pearson, R. G. *J. Am. Chem. Soc.* **1963**, *85*, 3533. Ahrland, S. *Struct. Bonding (Berlin)* **1968**, *5*, 118.

(27) Gomez-Romero, R.; Jameson, G. B.; Casan-Pastor, N.; Coronado, E.; Beltarn, D. *Inorg. Chem.* **1986**, *25*, 3171. Coronado, E.; Drillon, M.; Nugteren, P. R.; de Jongh, L. J.; Beltran, D.; Georges, R. *J. Am. Chem. Soc.* **1989**, *111*, 3874.

(23) Caneschi, A.; Gatteschi, D.; Melandri, M. C.; Rey, P.; Sessoli, R. *Inorg. Chem.* **1990**, *29*, 4228.

(24) Seiden, J. *J. Phys. Lett.* **1983**, *44*, L947.

pared to $\text{Mn}_2\text{M}(\text{hfac})_6(\text{NITpPy})_2$. The saturation magnetization in this case corresponds to $S = 5$. This value and the absence of any evidence of spin flipping in an external magnetic field agree with the structural model we have obtained. In fact the expected antiferromagnetic interaction between the radical and nickel(II) through the pyridine nitrogen⁹ leads to a parallel arrangement of nickel and manganese spins and to $S = 5$ for the formula unit. The magnetic phase transition occurs at higher temperature in III than in I in agreement with the larger magnetic moment of III compared to I.

Within this assumption the high-temperature susceptibility must be given by the sum of that of the manganese-radical chains of the side-pieces plus the contribution of an uncoupled nickel(II) ion. In fact χT could be fitted to give $J = 367$ (3) cm^{-1} . The difference between the J values estimated from the data of I and III is probably related to the different contribution of the off-chain metal ions which in I tends to reduce the susceptibility and in II tends to increase it.

The interpretation of the data for $\text{Mn}_2\text{Co}(\text{hfac})_6(\text{NITpPy})_2$ is complicated by the anticipated large anisotropy associated with the octahedral cobalt(II),²⁸ which is bound to unquenched orbital contributions. This anisotropy may be responsible for the different behavior of the ac susceptibility of II compared to I and III; however also in this case, the lack of metamagnetic behavior sug-

gests that the off-chains sites are essentially occupied by cobalt(II) ions.

Conclusions

The analysis of the magnetic properties of $\text{Mn}_2\text{M}(\text{hfac})_6(\text{NITpPy})_2$ allowed us to suggest a structure for these compounds. We think we have provided sound evidence that in these materials, chains $\text{Mn}(\text{hfac})_2(\text{NITpPy})$ are connected by $\text{M}(\text{py})_2$ groups. These compounds therefore provide examples of low dimensional materials in which three different spins regularly alternate in space. A possible description is that of regular bimetallic ribbons (or layers) in which the metal ions are bridged by tridentate NITpPy radicals. Our original goal was that of increasing the critical temperatures to three-dimensional order by cross-linking the $\text{Mn}(\text{hfac})_2(\text{NITR})$ chains. Although we have succeeded to some extent in connecting the chains, the critical temperatures have not increased.

Acknowledgment. Thanks are due to Professor A. C. Fabretti, University of Modena, for recording the IR spectra. The financial contributions of MURST and of Progetto Finalizzato Materiali Speciali per Tecnologie Avanzate are gratefully acknowledged.

Registry No. I, 137845-54-6; II, 137845-56-8; III, 137845-58-0.

Supplementary Material Available: Figure S1 and Figure S2 showing the temperature dependence of the magnetic susceptibility for $\text{Mn}_2\text{Co}(\text{hfac})_6(\text{NITpPy})_2$ and $\text{Mn}_2\text{Ni}(\text{hfac})_6(\text{NITpPy})_2$, respectively, and, in the inset of Figure S2, the calculated susceptibility. (2 pages). Ordering information is given on any current masthead page.

(28) Banci, L.; Bencini, A.; Benelli, C.; Gatteschi, D.; Zanchini, C. *Struct. Bonding (Berlin)* 1982, 52, 32.

Electrochemical Quartz Crystal Microbalance Monitoring of Cadmium Sulfide Generation in Polypyrrole and Polypyrrole Poly(styrenesulfonate) Thin Films

Maria Hepel,^{*1} Edith Seymour,¹ David Yogev,² and Janos H. Fendler^{*2}

Department of Chemistry, State University of New York at Potsdam, Potsdam, New York 13676, and Department of Chemistry, Syracuse University, Syracuse, New York 13244-4100

Received August 12, 1991. Revised Manuscript Received November 4, 1991

Cadmium sulfide, CdS, particles have been in situ generated electrochemically in polypyrrole, PPy, and polypyrrole-poly(styrenesulfonate), PPy/PSS⁻, composite thin films on a gold-coated quartz crystal electrode. Two different approaches have been taken. In the first approach, cadmium ions have been attached to the PPy/PSS⁻ composite thin film, formed upon subjecting an aqueous deoxygenated 2.0×10^{-2} M pyrrole solution to an $E = 0$ to $E = 600$ mV potential step in the presence of 1.0×10^{-3} M PSS⁻ and 0.10 M NaCl. Addition of cadmium ions followed by the introduction of bisulfide ions (HS⁻) has led to the formation of CdS particles at a number of nucleation sites. In the second approach, HS⁻ ions have been electrochemically oxidized to elementary sulfur in the matrices of PPy thin films, formed upon applying a potential step from $E = 0$ to $E = 650$ mV to an aqueous deoxygenated 2.0×10^{-2} M pyrrole solution in the presence of a 0.10 M NaCl supporting electrolyte. Subsequent to the removal of excess HS⁻ (by ion exchange by Cl⁻) cadmium ions have been added to the solution bathing the PPy-coated electrode. Cathodization has then reduced both the oxidized form of PPy and the elementary sulfur and has led to the formation of CdS particles at a large number of nucleation sites. Interfacial mass changes which have accompanied the formation of PPy and PPy/PSS⁻ thin films and CdS formation therein have been monitored by an electrochemical quartz crystal microbalance. Scanning electron microscopy and X-ray diffraction measurements have confirmed the presence of nonuniform CdS particles in the PPy and PPy/PSS⁻ films.

Introduction

Beneficial mechanical, optical, electrical, electrooptical, electrochemical, and chemical properties render conducting polymer-semiconductor heterojunctions to be useful in a

number of applications, including solar energy conversion.³⁻⁵ On the one hand, surface coating by polypyrrole

(1) State University of New York at Potsdam.

(2) Syracuse University.

(3) *Energy Resources through Photochemistry and Catalysis*; Grätzel, M., Ed.; Academic: New York, 1983.

(4) *Organic Phototransformations in Nonhomogeneous Media*; Fox, M. A., Ed.; American Chemical Society: Washington, DC, 1985.